Available online at www.sciencedirect.com
SCIENCE DIRECT®
International Journal of Heat and Mass Transfer 47 (2004) 3669–3681
International Journal of HEAT and MASS TRANSFER
www.elsevier.com/locate/ijhmt

Heat and mass transfer between gas and liquid streams in direct contact

K. Boulama [a], N. Galanis [a,*], J. Orfi [b]

[a] THERMAUS, Génie Mécanique, Université de Sherbrooke, Sherbrooke, QC, Canada J1K 2R1
[b] LESTE, École Nationale d'Ingénieurs de Monastir, Monastir 5019, Tunisia

Received 28 February 2003; received in revised form 2 April 2004
Available online 19 May 2004

Abstract

A one-dimensional model of heat and mass transfer between gas and liquid streams in direct contact within a duct has been solved using power series expansions for the unknown functions which describe the stream wise evolutions of the bulk temperatures, the mass ratio in the gas phase and the liquid mass flow rate. The model is based on the assumptions of constant heat and mass transfer coefficients and the existence of a thin saturated layer between the two streams. The solution can be used for any axially invariable geometrical configuration, for any combination of fluids and for laminar or turbulent flow conditions. It has been applied to air and water systems to investigate the effects of different entry conditions and adiabatic or non-adiabatic walls on the performance of evaporators and condensers with parallel or counter-flow arrangements.

Résumé

Un modèle unidimensionnel de transferts de chaleur et de masse entre un écoulement gazeux et un film liquide en contact direct dans une conduite a été solutionné en postulant une variation polynomiale pour les fonctions inconnues décrivant les évolutions axiales des températures moyennes, de la composition du gaz et du débit de liquide. Le modèle est basé sur les hypothèses de la constance des coefficients d'échanges de chaleur et de masse et de l'existence d'un film mince saturé à l'interface entre les écoulements gazeux et liquide. La solution peut être utilisée pour n'importe quelle géométrie d'échangeur, n'importe quelle combinaison de fluides et pour des régimes laminaire ou turbulent. Elle a été appliquée à des systèmes air-eau pour étudier les effets de différentes conditions d'entrée et des parois adiabatiques ou non adiabatiques sur les performances d'évaporateurs et condenseurs de type co- ou contre-courant.

1. Introduction

Simultaneous heat and mass transfer between a liquid and a gas in direct contact occurs in nature (wind over a lake, ...) and in many industrial applications (cooling towers, chemical vapour deposition processes, ...). It has therefore been the subject of many studies including an early analysis of laminar film condensation of saturated vapour on a vertical plate by Nusselt [1]. The more recent literature on flows with heat transfer and evaporation or condensation includes experimental [2–4] and numerical [5–9] studies with various combinations of liquids and gases for both external and internal flows, natural and mixed convection and two- and three-dimensional configurations. Numerical studies almost always use axially parabolic equations and neglect viscous dissipation of energy while, in many cases, the Boussinesq hypothesis and the

* Corresponding author. Tel.: +1-819-821-7144; fax: +1-819-821-7163.
E-mail address: nicolas.galanis@usherbrooke.ca (N. Galanis).

0017-9310/$ - see front matter © 2004 Elsevier Ltd. All rights reserved.
doi:10.1016/j.ijheatmasstransfer.2004.04.004

Nomenclature

C_p	specific heat at constant pressure [J kg^{-1} K^{-1}]
h	specific enthalpy [J kg^{-1}]
h_{fg}	specific enthalpy of evaporation [J kg^{-1}]
L	stream wise length of the exchanger [m]
Le	Lewis number ($Le = U_g/U_m(C_{p,A} + WC_{p,v})$)
$\dot{m}$	mass flow rate (kg s^{-1})
P'	span wise length of the liquid–gas interface [m]
P	span wise length of the interface between the wall and the liquid [m]
q_w	heat flux between liquid and wall [W m^{-2}]
T	temperature [°C]
U	coefficient of heat transfer [W m^{-2} K^{-1}]
U_m	coefficient of mass transfer [kg m^{-2} s^{-1}]
W	mass ratio ($W = m_v/m_A$) (kg of B/kg of A)
x	Axial coordinate (m)
X	Dimensionless axial coordinate ($X = xU_g/\dot{m}_A C_{p,A}$)

Greek symbol

ε	parameter indicating evaporation ($\varepsilon = 1$) or condensation ($\varepsilon = 0$)

Subscripts

A	first component of the gas mixture (non-soluble in the liquid)
B	second component of the gas mixture (condensable)
g	gas mixture
i	inlet conditions
l	liquid phase
s	saturated layer
v	vapour phase of component B

negligible liquid film thickness assumption are adopted. Nevertheless, the solution of these models require elaborate numerical schemes and considerable CPU time. Therefore, the published numerical studies present results for a few particular combinations of the controlling parameters which cannot be easily generalized. The same is true for experimental studies which require costly laboratory equipment and which pose considerable challenges regarding the control of the inlet conditions (in particular those of the liquid film).

Therefore, different simplified approaches have been proposed for modelling such double diffusion transfer phenomena. Thus, Minkowycz and Sparrow [10] studied analytically the laminar film condensation along an isothermal flat plate using a bi-dimensional boundary layer formulation. For internal flows, one-dimensional formulations with constant heat and mass transfer coefficients are used for the design and performance analysis of cooling towers and air humidifiers [11]. Perez-Blanco and Bird [12] also used a one-dimensional formulation with constant transfer coefficients and neglected span wise temperature differences within the liquid as well as second order differentials in the energy equation for the gas. Marseille et al. [13] improved this formulation by a correction equation in order to take into account the heat transfer between the liquid and the liquid–gas interface. Both these studies addressed counter-flow situations with evaporation and presented numerical solutions of the proposed models for some particular combinations of the independent parameters. Similar one-dimensional formulations and graphical solutions are included in heating, ventilating and air-conditioning textbooks such as the one by McQuiston et al. [14].

In this article we present a power series solution to the one-dimensional differential conservation equations for heat and mass transfer between gas and liquid streams in direct contact within a duct of arbitrary constant cross-section. The solution is obtained for both parallel- and counter-flow configurations with evaporation or condensation. Typical results for the stream wise variations of the bulk temperatures and average specific humidity for air–water flows together with a discussion on the effects of entering conditions on these variations are presented. Contrary to previous results, the present solution can be applied to any combination of the independent parameters for problems of heat and mass transfer between gas and liquid streams in direct contact.

2. Mathematical formulation

Fig. 1 shows a schematic cross-section of a duct of length L in which heat and mass are transferred across the interface P' between two streams in direct contact. The gas stream is a binary mixture of two non-reacting gases (small amount of B with large amount of A) in thermodynamic equilibrium. The bottom part of the duct contains a stream of component B in the liquid phase which may be flowing in the same or in the opposite direction as the gas mixture. Component A is not soluble in the liquid but mass transfer across the liquid–gas interface P' takes place by evaporation or condensation of component B. Sensible heat is also transferred across this interface which is augmented by the inclusion of the capillary strips partially immersed in the liquid stream.

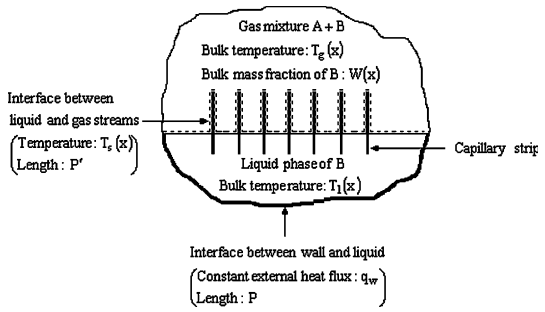

Fig. 1. Cross-sectional view of a heat and mass exchanger with direct contact between a binary gas mixture and a liquid (x coordinate perpendicular to figure).

The upper part of the duct (i.e. the interface between the duct wall and the gas mixture) is adiabatic. On the other hand, a uniform heat flux q_w is applied on the lower part of the duct (i.e. the interface between the duct wall and the liquid). The wall heat flux q_w, the cross-section geometry, as well as the lengths P and P' are considered to be constant over the entire length of the duct.

The gas stream enters the duct at $x = 0$ where its bulk temperature is $T_{g,i}$ and the average mass ratio of B (mass of B per mass of A) is W_i. The mass flow rate of component A at $x = 0$ is $\dot{m}_{A,i}$. The mass flow rate and bulk temperature of the liquid entering the duct (at $x = 0$ or $x = L$ for parallel- or counter-flow streams respectively) are $\dot{m}_{l,i}$ and $T_{l,i}$ respectively. The objective of the study is to calculate the axial evolutions of the two bulk temperatures $T_g(x)$ and $T_l(x)$, of the average mass ratio $W(x)$ and of the liquid mass flow rate $\dot{m}_l(x)$ for parallel- and counter-flow configurations.

The model for this steady-state heat and mass transfer problem is based on the existence of a very thin film of saturated gas between the liquid and gas streams. The temperature and mass ratio for this mass-less layer depend on the axial position but are related by the appropriate saturation relation:

$$W_s = W_s(T_s) \tag{1}$$

In the case of air and water for example, W represents the specific humidity and Eq. (1) corresponds to the line for 100% relative humidity on the psychrometric chart.

Conservation of mass for components A and B over the entire cross-section of the duct is expressed respectively by the following equations:

$$\dot{m}_A = \dot{m}_{A,i} \tag{2}$$

$$\dot{m}_A \frac{dW}{dx} \pm \frac{d\dot{m}_l}{dx} = 0 \tag{3}$$

In Eq. (3) and throughout this text the upper and lower signs correspond to parallel- and counter-flow configurations respectively.

Taking into account the mass flux between the thin saturated layer and the gas, conservation of mass for component B in the gas stream is expressed as follows:

$$\dot{m}_A \frac{dW}{dx} = U_m P'(W_s - W) \tag{4}$$

Concerning the heat transfer rates between the phases, it is first noted that Perez-Blanco and Bird [12] as well as the formulations in several HVAC textbooks [14] neglect the effect of thermal resistance in the liquid and thus set $T_s(x)$ equal to the corresponding bulk temperature of the liquid. Here we consider, as did Marseille et al. [13], that the saturated layer temperature $T_s(x)$ is different from both the bulk temperatures $T_g(x)$ and $T_l(x)$. Accordingly, the sensible heat fluxes from the saturated layer to the gas and liquid streams are proportional to the temperature differences $T_s(x) - T_g(x)$ and $T_s(x) - T_l(x)$ respectively. Therefore, energy conservation for the gas mixture, for the saturated film and for the liquid is expressed respectively by the following equations:

$$U_g P'(T_s - T_g) + \varepsilon \dot{m}_A \frac{dW}{dx}(h_s - h_B) = \dot{m}_A \left(\frac{dh_A}{dx} + W \frac{dh_B}{dx} \right) \tag{5}$$

$$U_g P'(T_g - T_s) + U_l P'(T_l - T_s) = \dot{m}_A \frac{dW}{dx}[\varepsilon(h_s - h_l) + (1 - \varepsilon)(h_B - h_s)] \tag{6}$$

$$U_l P'(T_s - T_l) + q_w P = \pm \dot{m}_l \frac{dh_l}{dx} \pm (1 - \varepsilon) \frac{d\dot{m}_l}{dx}(h_l - h_s) \tag{7}$$

In these last three equations the parameter ε is equal to unity in the presence of evaporation and to zero in the presence of condensation. The sum of these three equations expresses the global energy conservation over the entire cross-section of the duct and is independent of ε.

For counter-flow evaporation, Eqs. (3)–(7) reduce to those used in previously published articles and textbooks [12–14]. Perez-Blanco and Bird [12] as well as Marseille et al. [13] solved this system of differential equations numerically by means of a Runge Kutta scheme while the HVAC textbooks [14] used a graphical solution. To obtain these solutions it is assumed in all these studies that the heat and mass transfer coefficients U_g, U_l and U_m are constant. This assumption is also used in the present study, noting that it is analogous to the corresponding one used in the analysis of heat exchangers which leads to the generally accepted LMTD and effectiveness-NTU methods [1].

Eqs. (5)–(7) can be simplified using the following additional assumptions:

(i) The two components of the gas mixture are assumed to be ideal gases with constant properties (that is,

the specific heats at constant pressure are independent of temperature);

(ii) The subcooling of the liquid is assumed to be sufficiently small so that $h_s - h_l \approx h_{fg}$ in Eqs. (6) and (7) (consistently with the previous assumption, the enthalpy of vapourisation is considered to be constant).

With these assumptions, Eqs. (5)–(7) become:

$$U_g P'(T_s - T_g) + \varepsilon \dot{m}_A \frac{dW}{dx} C_{p,v}(T_s - T_g) = \dot{m}_A (C_{p,A} + W C_{p,v}) \frac{dT_g}{dx} \quad (5a)$$

$$U_g P'(T_g - T_s) + U_l P'(T_l - T_s) = \dot{m}_A \frac{dW}{dx} [\varepsilon h_{fg} + C_{p,v}(1-\varepsilon)(T_g - T_s)] \quad (6a)$$

$$U_l P'(T_s - T_l) + q_w P = \pm \dot{m}_l C_l \frac{dT_l}{dx} \mp (1-\varepsilon) \frac{d\dot{m}_l}{dx} h_{fg} \quad (7a)$$

The five differential equations (3), (4), (5a), (6a), (7a) together with relation (1) can be used to determine the unknown functions $T_g(x)$, $W(x)$, $\dot{m}_l(x)$, $T_l(x)$, $T_s(x)$ and $W_s(x)$. It should be noted that according to relation (2), the first two differential equations (3) and (4) are linear while the last three (5a), (6a) and (7a) contain products of the unknown functions.

The boundary conditions for this problem are:

$$T_g(x=0) = T_{g,i} \quad \text{and} \quad W(x=0) = W_i \quad (8)$$

and

$$T_l(x=0) = T_{l,i} \quad \text{and} \quad \dot{m}_l(x=0) = m_{l,i} \quad (9a)$$

for parallel-flow streams, or

$$T_l(x=L) = T_{l,i} \quad \text{and} \quad \dot{m}_l(x=L) = m_{l,i} \quad (9b)$$

for counter-flow streams.

3. Solution method

We assume that the unknown functions can be expressed as power series:

$$T_s = \sum_{j=0}^{\infty} a_j x^j, \quad W = \sum_{j=0}^{\infty} b_j x^j, \quad T_g = \sum_{j=0}^{\infty} d_j x^j,$$
$$\dot{m}_l = \sum_{j=0}^{\infty} f_j x^j \quad \text{and} \quad T_l = \sum_{j=0}^{\infty} g_j x^j \quad (10)$$

It is also assumed that the relation 1 between W_s and T_s can be approximated by a quadratic:

$$W_s = c_0 + c_1 T_s + c_2 T_s^2 \quad (1a)$$

The coefficients c_0, c_1, and c_2 are known constants obtained by a least square method from the exact corresponding values of W_s and T_s.

To compute the coefficients of the power series in Eq. (10), we first consider the boundary conditions. Thus, Eq. (8) together with the expressions of W and T_g give:

$$b_0 = W_i \quad \text{and} \quad d_0 = T_{g,i} \quad (11)$$

For parallel-flow streams, Eq. (9a) together with the expressions of $\dot{m}_l$ and T_l give:

$$f_0 = \dot{m}_{l,i} \quad \text{and} \quad g_0 = T_{l,i} \quad (12a)$$

or, alternatively, for counter-flow streams from Eq. (9b):

$$\sum_{j=0}^{\infty} f_j L^j = \dot{m}_{l,i} \quad \text{and} \quad \sum_{j=0}^{\infty} g_j L^j = T_{l,i} \quad (12b)$$

Combining the polynomial expression for T_s with Eq. (1a) and replacing the result as well as the polynomial expression for W in Eq. (4), we find:

$$b_1 = \frac{U_m P'}{\dot{m}_A}(c_0 + c_1 a_0 + c_2 a_0^2 - b_0) \quad (13a)$$

and

$$b_j = \frac{U_m P'}{j \dot{m}_A}[c_1 a_{j-1} + c_2(a_0 a_{j-1} + a_1 a_{j-2} + \cdots + a_{j-2} a_1 + a_{j-1} a_0) - b_{j-1}] \quad \text{for } j \geqslant 2 \quad (13b)$$

Similarly, by replacing the polynomial expressions for W and $\dot{m}_l$ in Eq. (3), we obtain:

$$f_j = \mp \dot{m}_A b_j \quad \text{for } j \geqslant 1 \quad (14)$$

Thus the expressions for b_j and f_j in terms of the known constants c_0, c_1, and c_2 and the as yet unknown coefficients a_j are the same for evaporation and condensation processes. On the other hand, the coefficients a_j, d_j and g_j which must be determined from Eqs. (5a), (6a) and (7a) depend on the value of the parameter ε. We must therefore distinguish two cases for their evaluation.

3.1. Heat transfer with evaporation

With $\varepsilon = 1$ Eqs. (5a), (6a) and (7a) become:

$$U_g P'(T_s - T_g) + \dot{m}_A \frac{dW}{dx} C_{p,v}(T_s - T_g) = \dot{m}_A (C_{p,A} + W C_{p,v}) \frac{dT_g}{dx} \quad (5b)$$

$$U_g P'(T_g - T_s) + U_l P'(T_l - T_s) = \dot{m}_A h_{fg} \frac{dW}{dx} \quad (6b)$$

$$U_l P'(T_s - T_l) + q_w P = \pm \dot{m}_l C_l \frac{dT_l}{dx} \quad (7b)$$

Eq. (6b) indicates that in this case the latent heat of evaporation is equal to the algebraic sum of the heat transferred to the saturated layer by the gas and by the liquid. It is also important to note that Eq. (7b) does not imply that the liquid mass flow rate $\dot{m}_l$ is constant (cf. Eq. (3)).

If the series expansions of T_s, W, T_g, $\dot{m}_l$ and T_l are replaced in (5b), (6b) and (7b) the following relations are obtained:

$$d_j = \frac{U_g P'(a_{j-1} - d_{j-1}) + \dot{m}_A C_{p,v}[b_1(a_{j-1} - d_{j-1}) + 2b_2(a_{j-2} - d_{j-2}) + \cdots + jb_j(a_0 - d_0)]}{j\dot{m}_A(C_{p,A} + WC_{p,v})} \quad \text{for } j \geqslant 1 \tag{15a}$$

$$g_1 = \frac{1}{f_0}\left[\pm\frac{U_l P'}{C_l}(a_0 - g_0) \pm \frac{q_w P}{C_l}\right] \tag{15b}$$

$$g_j = \frac{1}{jf_0}\left[\pm\frac{U_l P'}{C_l}(a_{j-1} - g_{j-1}) - (j-1)f_1 g_{j-1} - (j-2)f_2 g_{j-2} - \cdots - f_{j-1}g_1\right] \quad \text{for } j \geqslant 2 \tag{15c}$$

$$a_j = \frac{U_g P' d_j + U_l P' g_j - (j+1)\dot{m}_A h_{fg} b_{j+1}}{U_g P' + U_l P'} \quad \text{for } j \geqslant 0 \tag{15d}$$

It is interesting to note that the heat flux across the solid–liquid interface appears explicitly only in the expression for g_1 (Eq. (15b)). However, it indirectly influences all the other coefficients through Eqs. (15c), (15d), (15a), (13b) and (14) which clearly indicate the coupling between the three temperatures, the mass ratio of the gas mixture and the liquid mass flow rate.

Eqs. (11)–(15) can be used to calculate the coefficients of the power series defined in Eqs. (10) up to any required order j. Therefore, the axial evolutions of the temperatures, the mass ratio of the gas mixture and the liquid mass flow rate in a parallel- or counter-flow evaporator can be determined for any combination of the inlet conditions.

3.2. Heat transfer with condensation

With $\varepsilon = 0$ Eqs. (5a), (6a) and (7a) become:

$$U_g P'(T_s - T_g) = \dot{m}_A(C_{p,A} + WC_{p,v})\frac{dT_g}{dx} \tag{5c}$$

$$U_g P'(T_g - T_s) + U_l P'(T_l - T_s) = \dot{m}_A C_{p,v}\frac{dW}{dx}(T_g - T_s) \tag{6c}$$

$$U_l P'(T_s - T_l) + q_w P = \pm\dot{m}_l C_l \frac{dT_l}{dx} \mp \frac{d\dot{m}_l}{dx}h_{fg} \tag{7c}$$

In this case, the latent heat of condensation is distributed between three terms: heat transfer toward the saturated layer and across the solid–liquid interface as well as a variation of the liquid's internal energy. It is also important to note that Eq. (5c) does not imply that the mass ratio W is constant (cf. Eqs. (3) and (6c)).

If we replace the series expansions of T_s, W, T_g, $\dot{m}_l$ and T_l in (5c), (6c) and (7c), the following relations are obtained:

$$d_j = \frac{U_g P'(a_{j-1} - d_{j-1})}{j\dot{m}_A(C_{p,A} + WC_{p,v})} \quad \text{for } j \geqslant 1 \tag{16a}$$

$$g_1 = \frac{1}{f_0}\left[\pm\frac{U_l P'}{C_l}(a_0 - g_0) \pm \frac{q_w P}{C_l} + h_{fg}f_1\right] \tag{16b}$$

$$g_j = \frac{1}{jf_0}\left[\pm\frac{U_l P'}{C_l}(a_{j-1} - g_{j-1}) \pm j\frac{h_{fg}f_j}{C_l} - (j-1)f_1 g_{j-1} - (j-2)f_2 g_{j-2} - \cdots - f_{j-1}g_1\right] \quad \text{for } j \geqslant 2 \tag{16c}$$

$$a_j = \frac{U_g P' d_j + U_l P' g_j - \dot{m}_A C_{p,v}[(j+1)b_{j+1}d_0 + jb_j(d_1 - a_1) + \cdots + b_1(d_j - a_j)]}{U_g P' + U_l P' - \dot{m}_A C_{p,v} b_1} \quad \text{for } j \geqslant 0 \tag{16d}$$

It is again noted that the external heat flux q_w influences all the unknown variables despite the fact that it appears explicitly only in Eq. (16b).

Eqs. (11)–(14) and (16) can be used to determine the coefficients a_j, b_j, d_j, f_j and g_j up to any required order j. Therefore, the expressions for $T_s(x)$, $W(x)$, $T_g(x)$, $\dot{m}_l(x)$ and $T_l(x)$ defined by Eq. (10) can be determined for any parallel- or counter-flow condenser.

3.3. Solution procedure

All the thermophysical properties of the gas mixture and the liquid are evaluated at the known inlet conditions.

The values of the heat transfer coefficients U_l and U_g are evaluated from analytical results for different thermal boundary conditions [15] in the case of fully developed laminar flow or from heat transfer correlations [1] relating the Nusselt number to the Prandtl and Reynolds numbers in the case of developing or turbulent flow. The Reynolds number is calculated from the entering liquid or gas mass flow rates and the particular geometry under consideration (Fig. 1).

The value of the mass transfer coefficient U_m can be evaluated analogously based on the Schmidt and Reynolds numbers. Alternatively, it can be calculated from the heat transfer coefficient if the Lewis number is known.

The decision on whether to use the relations for evaporation or for condensation can be based on a comparison of the entering mass ratio of the gas mixture W_i with the corresponding saturation value at the entering liquid temperature. If $W_i < W_s(T_{l,i})$ evaporation is expected while if the opposite is true condensation will almost certainly occur. In case of doubt, a guess on one or the other of the two options is made. If it is not the right one, the calculations lead to physically unacceptable results.

The values of the coefficients in Eq. (10) can be calculated for any given combination of the 11 independent variables $\dot{m}_a$, $T_{g,i}$, W_i, $\dot{m}_{l,i}$, $T_{l,i}$, P, P', q_w, U_g, U_l and U_m with a simple spreadsheet. In the present case, using excell and a Pentium IV PC, graphical representations of the dependent functions $T_g(x)$, $W(x)$, $T_s(x)$, $T_l(x)$, $\dot{m}_l(x)$ were generated in less than 3 s.

4. Validation of the proposed solution

4.1. Comparison with analytical solution for simple heat exchangers

The case of heat transfer without mass transfer is represented by simply setting the coefficient of mass transfer U_m equal to zero in Eq. (4). Then Eqs. (3) and (4) indicate that both gas and liquid mass flow rates are constant and Eqs. (5a), (6a), (7a) become:

$$U_g P'(T_s - T_g) = \dot{m}_A(C_{p,A} + WC_{p,v})\frac{dT_g}{dx} \tag{17a}$$

$$U_g P'(T_g - T_s) + U_l P'(T_l - T_s) = 0 \tag{17b}$$

$$U_l P'(T_s - T_l) + q_w P = \pm \dot{m}_l C_l \frac{dT_l}{dx} \tag{17c}$$

These equations are the standard energy conservation equations for parallel- or counter-flow (positive or negative sign in Eq. (17c) respectively) heat exchangers with external heat transfer to one of the two fluids. For this situation T_s represents the temperature of the solid interface separating the two fluids. In this case, without mass transfer, both fluids can be liquids or gases. The exact solution to this system of three equations is:

$$T_l = A\exp(-\xi x) + \varphi x + B \tag{18a}$$

where

$$\xi = \frac{U_g P' U_l}{U_g + U_l}\left(\frac{\dot{m}_l C_l \pm \dot{m}_A(C_{p,A} + WC_{p,v})}{\dot{m}_l C_l \dot{m}_A(C_{p,A} + WC_{p,v})}\right) \tag{18b}$$

and

$$\varphi = \frac{q_w P}{\dot{m}_A(C_{p,A} + WC_{p,v}) \pm \dot{m}_l C_l} \tag{18c}$$

This general form is always valid except for the particular case of a counter-flow heat exchanger with equal liquid and gas heat capacity rates.

The constants A and B depend on the flow configuration. For parallel-flow, for which $T_g(x=0) = T_{g,i}$ and $T_l(x=0) = T_{l,i}$, their expressions are:

$$A = \frac{1}{\xi}\left[\frac{(T_{l,i} - T_{g,i})}{\dot{m}_l C_l}\frac{U_g P' U_l}{U_g + U_l} + \varphi - \frac{q_w P}{\dot{m}_l C_l}\right] \tag{18d}$$

$$B = T_{l,i} - A \tag{18e}$$

For counter-flow, for which $T_g(x=0) = T_{g,i}$ and $T_l(x=L) = T_{l,i}$, they are:

$$A = \frac{T_{g,i} - T_{l,i} + \varphi\left[L + \dot{m}_l C_l \frac{U_g + U_l}{U_g P' U_l}\right] + q_w P \frac{U_g + U_l}{U_g P' U_l}}{1 - \exp(-\xi L) + \dot{m}_l C_l\left(\frac{U_g + U_l}{U_g P' U_l}\right)\xi} \tag{18f}$$

and

$$B = T_{l,i} - A\exp(-\xi L) - \varphi L \tag{18g}$$

The temperatures of the second fluid and of the interface are given by the following expressions:

$$T_g = T_l + \frac{U_g + U_l}{U_g P' U_l}\left(\pm \dot{m}_l C_l \frac{dT_l}{dx} - q_w P\right) \tag{19}$$

$$T_s = \frac{U_g T_g + U_l T_l}{U_g + U_l} \tag{20}$$

This exact solution can be compared with the corresponding series expansion solution derived in the previous section of the paper. By putting $U_m = 0$ in Eq. (13), the coefficients of Eq. (10), as given either by the relations (11)–(15) (for evaporation) or by the relations (11)–(14) and (16) (for condensation), become:

$$b_j = f_j = 0 \quad \text{for } j \geqslant 1 \tag{21a}$$

$$d_j = \frac{U_g P'(a_{j-1} - d_{j-1})}{j\dot{m}_A(C_{p,A} + WC_{p,v})} \quad \text{for } j \geqslant 1 \tag{21b}$$

$$g_1 = \frac{1}{f_0}\left[\pm\frac{U_l P'}{C_l}(a_0 - g_0) \pm \frac{q_w P}{C_l}\right] \tag{21c}$$

$$g_j = \frac{1}{jf_0}\left[\pm\frac{U_l P'}{C_l}(a_{j-1} - g_{j-1})\right] \quad \text{for } j \geqslant 2 \tag{21d}$$

$$a_j = \frac{U_g d_j + U_l g_j}{U_g + U_l} \quad \text{for } j \geqslant 0 \tag{21e}$$

Eqs. (21a) indicate that the mass flow rates of the two fluids are constant as expected. The temperatures of the two fluids and of the interface are calculated from Eq. (10) using the boundary conditions (11) and (12) together with Eqs. (21b), (21c), (21d) and (21e).

Fig. 2 shows a comparison of the axial temperature evolutions in a parallel- (Fig. 2a) and in a counter-flow

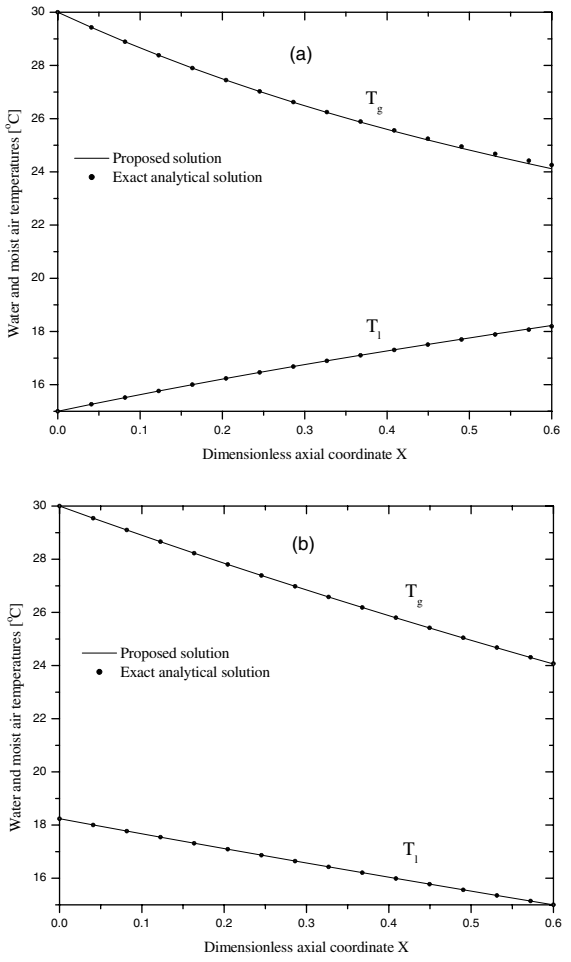

Fig. 2. Validation of the proposed model: (a) parallel-flow heat exchanger, (b) counter-flow heat exchanger.

(Fig. 2b) heat exchanger obtained from the exact solution (Eqs. (18)–(20)) and the power series expansions (Eqs. (10)–(12) and (21)). For this comparison the hot and cold fluids are moist air ($T_{g,i} = 30$ °C and $W_i = 0.02$) and water ($T_{l,i} = 15$ °C) respectively. The mass flow rates of dry air and water are equal ($\dot{m}_A = \dot{m}_{l,i} = 0.1$ kg/s) and a uniform external heat flux ($q_w = 100$ W/m^2) is supplied to the water. The Nusselt numbers for the water and air flows are set equal to 4.0 and 4.86 respectively. These are the Nusselt numbers for fully developed laminar flow in channels with, in the first case, an adiabatic and an isothermal boundary and, in the second case, an isothermal and a uniform heat flux boundary [15]. The geometrical variables for this validation are $P = 1$ m, $P' = 10$ m and the exchanger cross-section is rectangular (1 m by 0.1 m). The power series in Eq. (10) were truncated after x^3 (i.e. the coefficients of x^j are equal to zero for $j \geqslant 4$). The agreement between the two solutions is excellent in both parallel- and counter-flow configurations over the entire length of the heat exchanger (the maximum error committed is less than 0.6%).

Equally good agreement between the exact solution and the power series expansions has been obtained for other operating conditions with different fluid combinations and both parallel- and counter-flow configurations. We therefore consider that the third order power series expansions provide sufficiently accurate representations of the axial evolution of the bulk temperatures for any such heat exchanger.

4.2. Comparison with published results for heat and mass transfer

Based on the results of the previous section, we assume that the third order power series expansions can be used to represent the axial evolutions of bulk temperatures, liquid mass flow rate and mass ratio of the gas phase for the parallel- and counter-flow heat and mass transfer installations such as the one schematized in Fig. 1. Validation of the proposed model and the truncated power series solution for cases with both heat and mass transfer between humid air and a moving water film is provided in Fig. 3. It presents the axial evolutions of T_s and W predicted by the present method and corresponding results by Yan [16] who solved the two-dimensional partial differential equations to evaluate the effect of evaporation on laminar mixed convection in a vertical parallel plate channel. This numerical study is one of the relatively few which considers a finite liquid film thickness and shows very clearly that the assumption of the negligible liquid film thickness is inappropriate, especially near the channel entrance, for high liquid mass flow rates. The values predicted by the present analytical solution were calculated with $Nu_g = 4.86$ and $Nu_l = 4.0$. For Fig. 3 the Reynolds number and hydraulic diameter are such that the length of the channel is 3 m. The results show that the temperatures predicted by the present method are in very good agreement with Yan's results, particularly in the first 2 m of the channel. In the case of the specific humidity (Fig. 3b), the two methods predict similar qualitative results but the numerical values differ by as much as 10%. In view of the complexity of the problem and the number of differing assumptions used by the two studies, we consider that the overall agreement is acceptable.

4.3. Other tests

In order to further evaluate the proposed model and its power series solution, several tests have been performed for easily predictable limiting cases. Thus, for example, for an air–water combination with $T_{g,i} = T_{l,i} = 15$ °C, $W_i = W_s$ (15 °C), $\dot{m}_a = \dot{m}_{l,i} = 0.1$ kg/s and $q_w = 0$, the truncated power series for both evaporation and

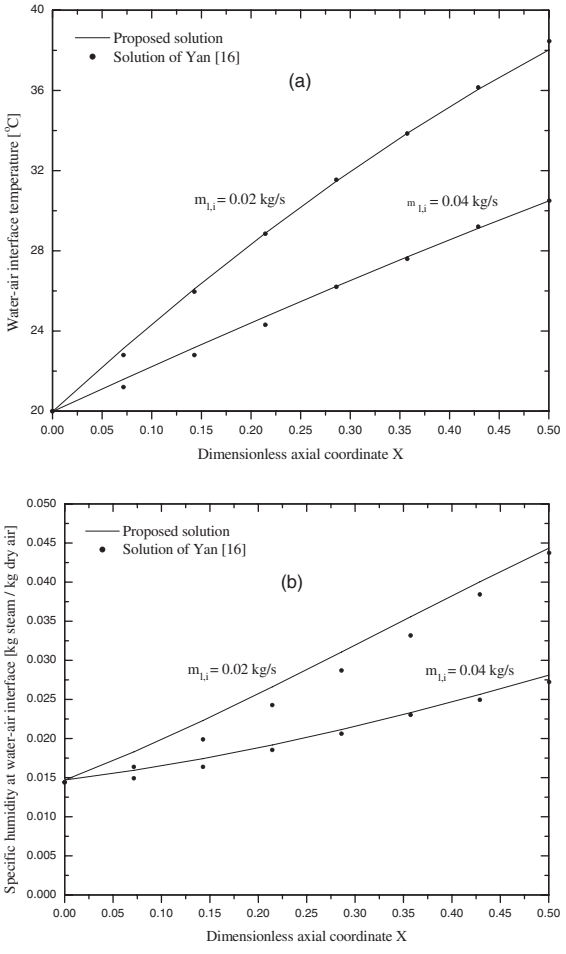

Fig. 3. Validation of the proposed model for parallel-flow with heat and mass transfer.

condensation result in $T_g(x) = T_l(x) = T_s(x) = 15$ °C, $\dot{m}_l(x) = 0.1$ kg/s and $W(x) = W_s$ (15 °C) within 6 significant figures for $0 \leqslant x \leqslant 6$ m. This and other similar results indicate the precision and stability of the third order truncated power series.

5. Application to air and water streams

Simultaneous heat and mass transfer between air and water occurs in many situations of practical interest. This combination of fluids is therefore used to illustrate the application of the truncated power series solution by investigating the effects of different entry conditions on the axial evolution of the specific air humidity and of the bulk temperatures. It should be noted that for these calculations we have assumed that the duct is rectangular with a height of 0.1 m and $P' = 10P = 10$ m, that $Nu_g = 4.86$, $Nu_l = 4.0$ and $Le = 0.9$. The saturation conditions (Eq. (1) or (1a)) for the temperature range under consideration ($8 \leqslant T \leqslant 44$ °C) and standard atmospheric pressure are approximated by:

$$W_s = (7.17 - 0.29T + 0.0333T^2)10^{-2}$$

where T is in °C and W_s is in kg of vapour per kg of dry air.

5.1. Heat exchanger with evaporation

Fig. 4a and b illustrate the effect of the mass flow rate ratio ($\dot{m}_{l,i}/\dot{m}_A$) on the performance of an adiabatic ($q_w = 0$) parallel-flow evaporator using warm dry air ($T_{g,i} = 35$ °C and $W_i = 0.005$) and cool water ($T_{l,i} = 15$ °C). Predictably, as the fluids move downstream, their temperatures tend towards an intermediate value and the air humidity increases (Fig. 4a). The temperature of the saturated layer T_s varies similarly to that of the liquid

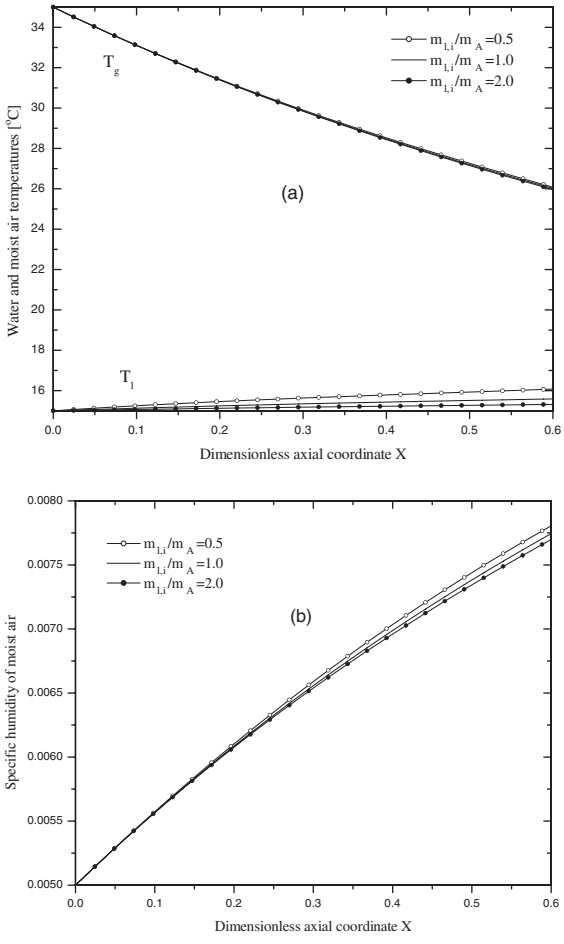

Fig. 4. Effects of mass flow rate ratio at inlet on the performance of an adiabatic parallel-flow heat and mass exchanger with evaporation.

T_l and is not shown in the figure because it is very close to the latter. Near the inlet the rate of evaporation, which is proportional to the slope of $W(x)$, is the same for all cases (Fig. 4b). Further downstream however, the rate of evaporation increases as $\dot{m}_{l,i}/\dot{m}_A$ decreases. The liquid mass flow rate decreases monotonically with x as expected. Since its decrease over the entire length of the exchanger is very small, $\dot{m}_l(x)$ has not been plotted. Fig. 4a also shows that when $\dot{m}_{l,i}/\dot{m}_A$ decreases the temperature of the water stream increases while that of the air stream increases very slightly. It is obvious from these results that, for the conditions under consideration, the air supplies both the latent heat of evaporation corresponding to the increase of the specific humidity and the sensible heat corresponding to the temperature increase of the liquid. Finally the differences observed on Fig. 4a and b when different mass flow rate ratios are considered confirm the necessity to take into account the presence and movement of the liquid film rather than assuming that its thickness is negligible.

Fig. 5a and b illustrate the effect of the inlet liquid temperature on the performance of an adiabatic parallel-flow evaporator with $\dot{m}_A = \dot{m}_{l,i} = 0.1$ kg/s and $W_i = 0.005$ kg steam/kg air. For these calculations, the inlet temperature difference $\Delta T = T_{g,i} - T_{l,i}$ was held constant and equal to 20 °C. The results represented in Fig. 5a show that the air temperature change between the inlet and outlet increases slightly as $T_{l,i}$ increases. The same tendency applies to the sensible heat transfer from the gas stream. In the liquid film a rather unexpected phenomenon occurs. As the axial coordinate x increases, the liquid temperature increases for $T_{l,i} = 15$ °C but decreases for $T_{l,i} = 25$ °C. So, in the former case sensible heat is supplied to the liquid while in the latter case it is lost by the liquid. In Fig. 5b, it can be seen that the rate of evaporation is always higher near the inlet and increases considerably with increasing entering liquid temperature. These results indicate that for low values of $T_{l,i}$ the air supplies the latent heat necessary for the evaporation as well as the sensible heat to increase the temperature of the liquid. On the other hand, for higher values of $T_{l,i}$, the latent heat of evaporation is supplied by both fluids. The previous observations concerning $T_s(x)$ and $\dot{m}_l(x)$ apply again.

Fig. 6a and b illustrate the effect of the inlet air humidity on the performance of a parallel-flow adiabatic evaporator. During this analysis entering temperatures and mass flow rates of water and dry air were kept constant ($\dot{m}_A = \dot{m}_{l,i} = 0.1$ kg/s, $T_{l,i} = 15$ °C and $T_{g,i} = 35$ °C). It is seen (Fig. 6b) that the rate of evaporation decreases considerably as W_i increases. Since a smaller rate of evaporation implies a reduced latent heat flux, the net sensible heat transfer to the water film increases and the cooling effect on the moist air stream is worsened (Fig. 6a).

The effects of wall heating and those of the flow arrangement (parallel- or counter-flow exchanger) on

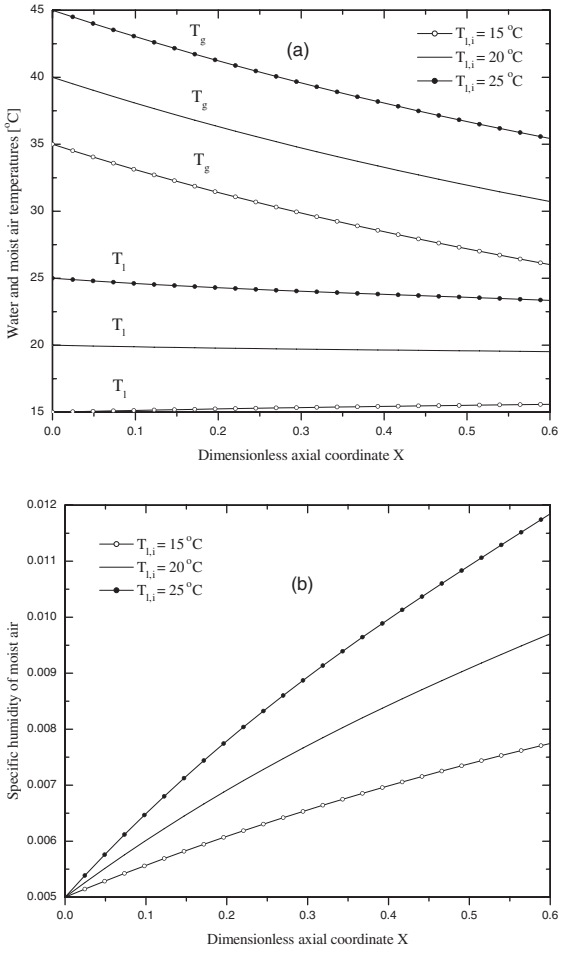

Fig. 5. Effects of water temperature at inlet on the performance of an adiabatic parallel-flow heat and mass exchanger with evaporation.

the transfer phenomena have also been investigated but are not presented for lack of space. For the combinations of variables in Figs. 4–6, it has been shown that when a uniform heat flux is supplied to the liquid, both air and water temperatures as well as the evaporation rate increase. However, the effect on T_l is greater than that on T_g. On the other hand, the counter-flow configuration results in different local heat and mass fluxes but has a rather small beneficial effect on the overall change of the temperatures and specific humidity. This result is qualitatively similar to the small performance improvement of heat exchangers with low NTU values [1].

5.2. Heat transfer with condensation

Fig. 7a and b illustrate the effect of the mass flow rate ratio $(\dot{m}_{l,i}/\dot{m}_A)$ on the performance of an adiabatic

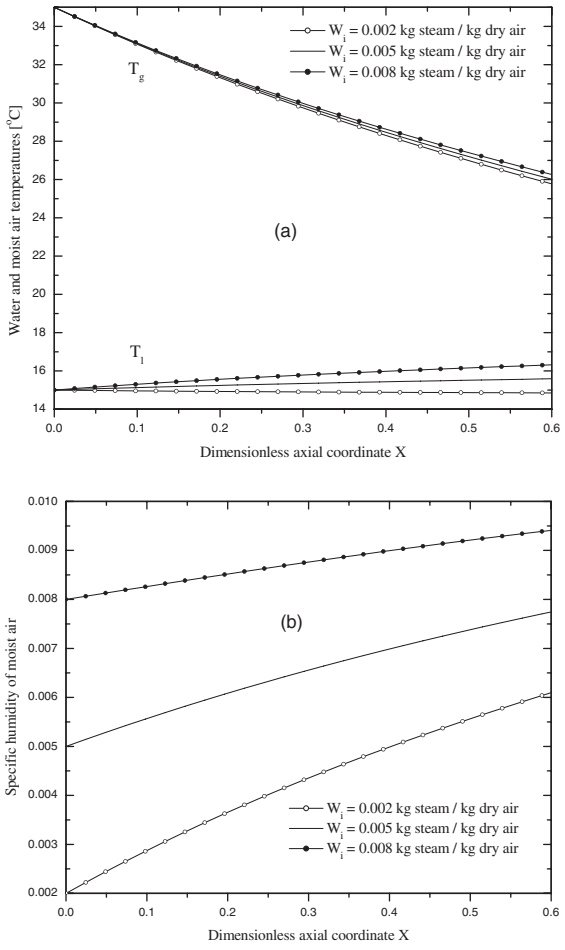

Fig. 6. Effects of vapour mass fraction in the entering moist air on the performance of an adiabatic parallel-flow heat and mass exchanger with evaporation.

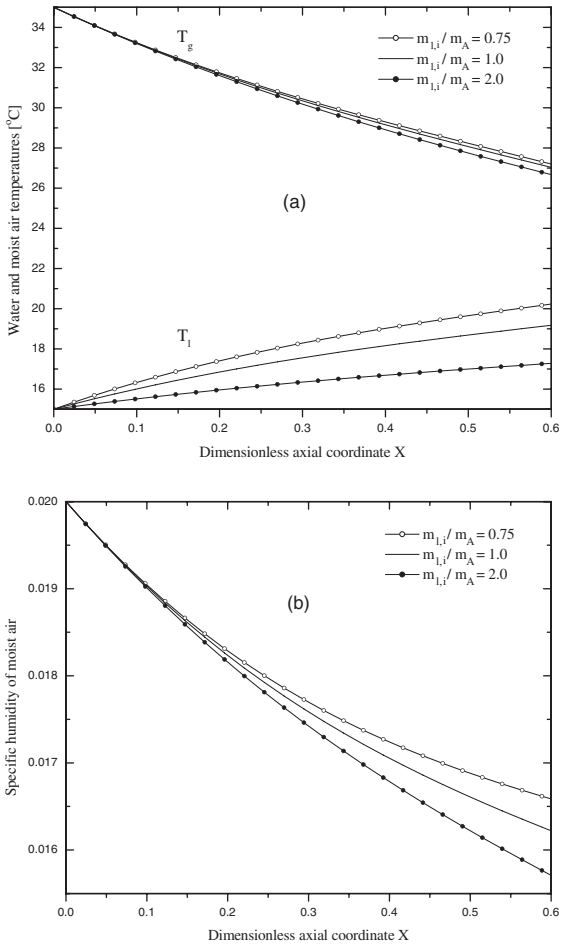

Fig. 7. Effects of mass flow rate ratio at inlet on the performance of an adiabatic parallel-flow heat and mass exchanger with condensation.

($q_w = 0$) parallel-flow condenser using warm humid air ($T_{g,i} = 35$ °C and $W_i = 0.02$) and cool water ($T_{l,i} = 15$ °C). As expected, the two temperatures tend towards an intermediate value and the vapour mass ratio in the gas phase decreases. It is noted that the sensible heat transfer from the air stream and the rate of condensation increase with $\dot{m}_{l,i}/\dot{m}_A$. However, since the latter increases faster than the former, less sensible heat (per kilogram per second) is transferred to the water when $\dot{m}_{l,i}/\dot{m}_A$ increases. Therefore the temperature change of the water decreases as $\dot{m}_{l,i}/\dot{m}_A$ increases. The important effect of the mass flow rate ratio on the liquid temperature change (Fig. 7a) and on the specific humidity change (Fig. 7b) confirms, once again, the necessity of taking into account the presence and the movement of the liquid film.

Fig. 8a and b illustrate the effect of the inlet liquid temperature on the performance of an adiabatic parallel-flow condenser with $\dot{m}_A = \dot{m}_{l,i} = 0.1$ kg/s and $W_i = 0.025$ kg steam/kg dry air. For these calculations the inlet temperature difference $\Delta T = T_{g,i} - T_{l,i}$ was held constant and equal to 20 °C. The results shown in Fig. 8a indicate that, when the entering water temperature increases, the sensible heat transfer to the water stream decreases slightly without any significant effect on the evolution of the air temperature. On the other hand, Fig. 8b indicates that the rate of condensation decreases considerably when water enters the exchanger with high temperatures. The relative effects on $T_l - T_{l,i}$ and $W_i - W$ are consistent with an overall energy balance which indicates that these quantities are inversely proportional to $\dot{m}_{l,i}C_{l,i}$ and $\dot{m}_a h_{fg}$ respectively.

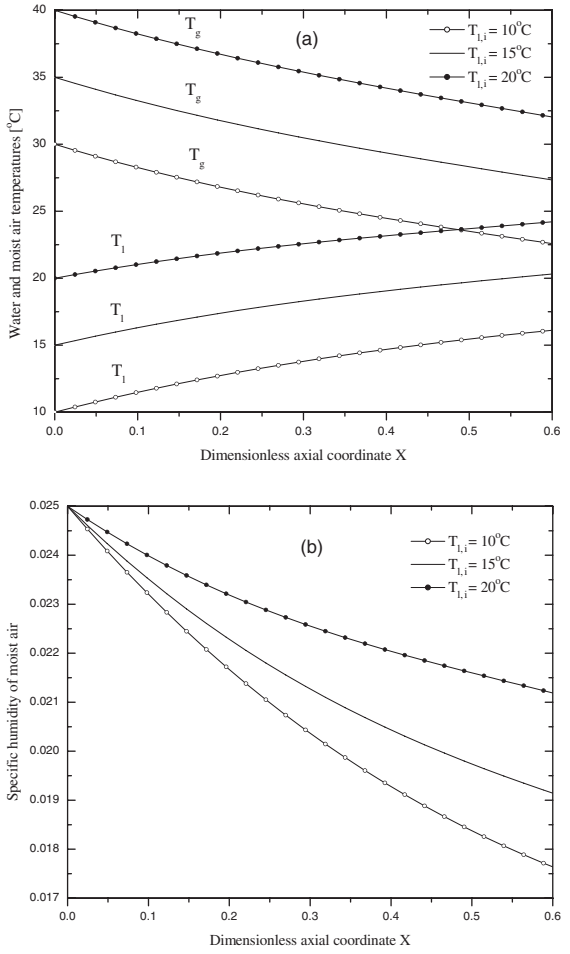

Fig. 8. Effects of water temperature at inlet on the performance of an adiabatic parallel-flow heat and mass exchanger with condensation.

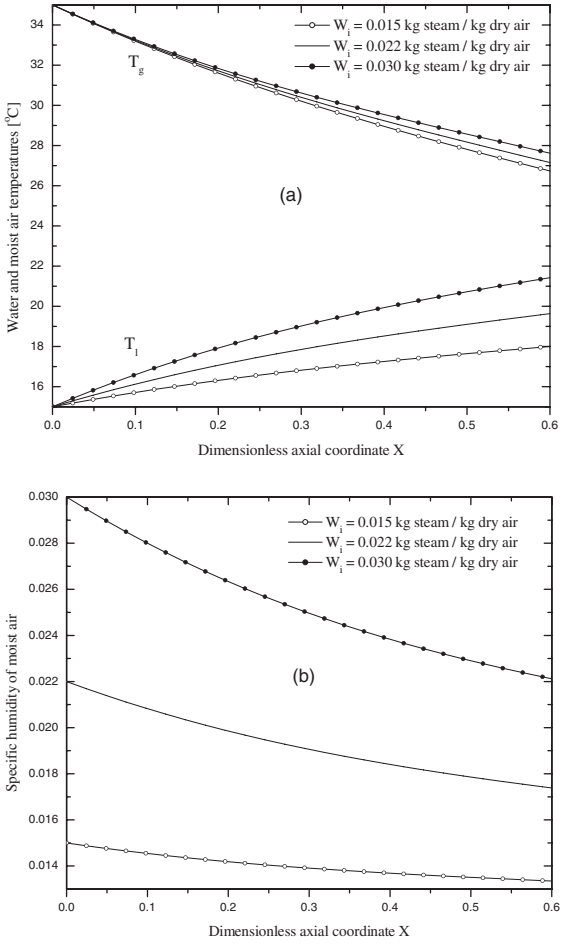

Fig. 9. Effects of vapour mass fraction in the entering moist air on the performance of an adiabatic parallel-flow heat and mass exchanger with condensation.

Fig. 9a and b illustrate the effect of the inlet air humidity on the performance of a parallel-flow adiabatic heat and mass exchanger in the presence of condensation. The entering temperatures and mass flow rates of water and dry air are kept constant ($T_{l,i} = 15$ °C, $T_{g,i} = 35$ °C and $\dot{m}_A = \dot{m}_{l,i} = 0.1$ kg/s) and different values of W_i are considered. Fig. 9b shows that the rate of condensation increases as W_i increases, thus providing more and more latent heat to both the air and water streams. By so doing, the increase of W_i enhances the heating of the water stream and reduces the cooling of the air stream (Fig. 9a).

As in the case of evaporation, the interface temperature $T_s(x)$ is very slightly higher than that of the liquid and the change of $\dot{m}_l$ from the inlet to the outlet of the duct is very small in all the investigated situations. Therefore these variables are not plotted in the paper.

The effects of wall cooling and flow arrangement have also been investigated. In all cases, it has been found, that when a uniform negative heat flux is applied on the bottom wall, both the air and water temperatures decrease while the condensation rate increases. The effect of the flow arrangement is the same as that discussed in the preceding section.

6. Conclusion

The proposed one-dimensional model for the study of heat and mass transfer between gas and liquid streams

in direct contact is based on the assumptions of constant fluid properties and constant transfer coefficients, identical to those used for the analysis of heat exchangers. It takes into account the presence and movement of the liquid film, which have been neglected in many two- and three-dimensional numerical studies despite its proven influence on heat and mass transfer rates. It also takes into account temperature differences in the liquid perpendicular to its flow direction, which had been neglected in previous one-dimensional studies.

The proposed power series solution has not been previously applied to this problem. Its truncated approximation has been successfully validated by comparisons with the analytical solution for a simple heat exchanger and with CFD results for a heated direct contact evaporator. It can be used for any axially invariable geometry, for any gas–liquid combination, for parallel- and counter-flow configurations, for evaporators or condensers, for adiabatic or uniformly heated solid–liquid interfaces, as well as for laminar and turbulent flow conditions (by an appropriate choice of transfer coefficients). Since its application is simple and does not require sophisticated or costly equipment, it is more useful than the results of previously published experimental and numerical studies which describe the performance of such heat and mass transfer processes for a particular combination of the independent parameters.

The application of the model and its truncated power series solution to air–water systems illustrates their flexibility. These results indicate that entering water temperature and specific air humidity greatly influence the heat and mass transfer rates in a direct contact evaporator. Their effects on the sensible heat transfer from the gas is always small while the sensible heat transfer to the liquid stream significantly increases and the evaporation rate decreases when the entering water temperature decreases or when the specific humidity of the entering moist air increases. Entering water temperature, specific humidity of the entering moist air and the mass flow rate ratio also influence the transfer rates in a direct contact condenser. In fact, the condensation rates and the heat transfer to the liquid stream decrease when the entering liquid temperature is raised and increase as the entering air humidity increases. Raising the ratio of liquid to dry air mass flow rates also contributes to enhance the condensation process but reduces the sensible heat transfer to the liquid stream. In all cases, the effect on the gas side sensible heat transfer is less significant.

Wall cooling or heating are also shown to have significant effects on the transfer phenomena. Conversely, flow arrangement has no major effect for the conditions of this study.

Acknowledgements

The support of this work by the Natural Sciences and Engineering Research Council of Canada is gratefully acknowledged.

References

[1] F.P. Incropera, D.P. DeWitt, Fundamentals of Heat and Mass Transfer, fifth ed., Wiley, New York, 2001.
[2] M. Haji, L.C. Chow, Experimental measurement of water evaporation rates into air and superheated steam, ASME Trans., J. Heat Transfer 110 (1988) 237–242.
[3] Y.L. Tsay, T.F. Lin, W.M. Yan, Cooling of a falling liquid film through interfacial heat and mass transfer, Int. J. Multiphase Flow 16 (1990) 853–865.
[4] W.M. Yan, T.F. Lin, Y.L. Tsay, Evaporative cooling of liquid film through interfacial heat and mass transfer in a vertical channel—I. Experimental study, Int. J. Heat Mass Transfer 34 (1991) 1105–1111.
[5] L.C. Chow, J.N. Chung, Evaporation of water into a laminar stream of air and superheated steam, Int. J. Heat Mass Transfer 26 (1983) 373–380.
[6] A. Agunaoun, M. Kaoua, A. Daïf, M. Daguenet, Évaporation en convection mixte d'un film liquide d'un mélange binaire s'écoulant sur un plan incliné soumis à un flux de chaleur constant, Int. J. Heat Mass Transfer 41 (1988) 2197–2210.
[7] A. Ali Cherif, A. Daïf, Étude numérique du transfert de chaleur et de masse entre deux plaques planes verticales en présence d'un film binaire ruisselant sur l'une des plaques chauffée, Int. J. Heat Mass Transfer 42 (1999) 2399–2418.
[8] C. Debbissi, J. Orfi, S. Ben Nasrallah, Evaporation of water by free convection in a vertical channel including effects of wall radiative properties, Int. J. Heat Mass Transfer 44 (2001) 811–826.
[9] J. Orfi, N. Galanis, Developing laminar mixed convection with heat and mass transfer in horizontal and vertical tubes, Int. J. Therm. Sci. 41 (2002) 319–331.
[10] W.J. Minkowycz, E.M. Sparrow, Condensation heat transfer in the presence of noncondensables, interfacial resistance, superheating, variable properties, and diffusion, Int. J. Heat Mass Transfer 9 (1966) 1125–1144.
[11] ASHRAE, Handbook of Fundamentals, Atlanta, 2001 (Chapter 5).
[12] H. Perez-Blanco, W.A. Bird, Study of heat and mass transfer in a vertical-tube evaporative cooler, ASME Trans, J. Heat Transfer 106 (1984) 210–215.
[13] T.J. Marseille, J.S. Schliesing, D.M. Bell, B.M. Johnson, Extending cooling tower thermal performance—prediction using a liquid–side film resistance model, Heat Transfer Eng. 12 (1991) 19–30.
[14] F.C. McQuiston, J.D. Parker, J.D. Spitler, Heating, Ventilating and Air Conditioning: Analysis and Design, fifth ed., Wiley, New York, 2000 (Chapter 13).

[15] S. Kakaç, R.K. Shah, W. Aung, Handbook of Single-Phase Convective Heat Transfer, Wiley, New York, 1987.

[16] W.M. Yan, Effects of film evaporation on laminar mixed convection heat and mass transfer in a vertical channel, Int. J. Heat Mass Transfer 35 (1992) 3419–3429.